

## Variational Field Theoretic Approach to Relativistic Scattering

C. Alexandrou<sup>1,2</sup>, R. Rosenfelder<sup>2</sup> and A. W. Schreiber<sup>2,3,4</sup>

<sup>1</sup> Department of Natural Sciences, University of Cyprus, CY-1678 Nicosia, Cyprus

<sup>2</sup> Paul Scherrer Institute, CH-5232 Villigen PSI, Switzerland

<sup>3</sup> TRIUMF, 4004 Wesbrook Mall, Vancouver, B.C., Canada V6T 2A3

<sup>4</sup> Department of Physics and Mathematical Physics and Research Centre for the Subatomic Structure of Matter, University of Adelaide, Adelaide, S. A. 5005, Australia

### Abstract

Nonperturbative polaron variational methods are applied, within the so-called particle or worldline representation of relativistic field theory, to study scattering in the context of the scalar Wick - Cutkosky model. Important features of the variational calculation are that it is a controlled approximation scheme valid for arbitrary coupling strengths, the Green functions have all the cuts and poles expected for the exact result at any order in perturbation theory and that the variational parameters are simultaneously sensitive to the infrared as well as the ultraviolet behaviour of the theory. We generalize the previously used quadratic trial action by allowing more freedom for off-shell propagation without a change in the on-shell variational equations and evaluate the scattering amplitude at first order in the variational scheme. Particular attention is paid to the  $s$ -channel scattering near threshold because here non-perturbative effects can be large. We check the unitarity of our numerical calculation and find it greatly improved compared to perturbation theory and to the zeroth order variational results.

# 1. Introduction

Variational techniques are widely used in the study of quantum mechanical systems. Most of these applications are based on the Rayleigh - Ritz variational principle for the energy of the system and physical intuition plays a crucial role in the construction of the variational wave function which is used. Applications of similar techniques to relativistic quantum field theories are, in contrast, rather limited. Intuitive arguments are hampered by having to deal with infinitely many degrees of freedom and the problem is further complicated by the need for renormalization. However, a well known example of a non-relativistic field theory where the variational approach has been highly successful is the polaron problem in condensed matter physics [1, 2]. Here it yields results within a few % compared to exact Monte Carlo results [3]. The main idea on which this success is based is the exact integration of the phonon degrees of freedom, thus obtaining an effective one-body system where an intuitive construction of a trial action is possible. The same approach has been applied to the Walecka model to study the one- [4] as well as many- [5] nucleon system.

The generalization of this method to relativistic theories is possible and forms the basis of the work described in this paper. It should be stressed that this is a variational method which is not related to the usual variational approach in quantum field theory, the latter using trial wave functionals of the field in order to obtain an approximation to the effective action (see [6] and references therein). Exact elimination of the light degrees of freedom (analogous to the phonons in the polaron problem) remains a central idea in this application. Furthermore, it is useful to employ the *particle* or *worldline* representation [2, 7 - 10] for the remaining heavy degrees of freedom of the theory. This formulation employs particle trajectories, parameterized in terms of a proper time, rather than local fields. Through its use the relativistic theory bears a startling similarity to the non-relativistic polaron problem and so it is not unreasonable to expect that some of the success enjoyed by the variational method so far will be repeated.

In a recent series of papers [11-14] (henceforth referred to as I - IV) we developed the variational treatment of a simplified field theory of two scalar interacting particles. The Lagrangian of this theory is of the Wick-Cutkosky type [15, 16] with a finite meson mass. As such, it has the same type of interaction as Lagrangians relevant to physical situations, for example any meson-nucleon theory or, in the limit of zero-mass, Quantum Electrodynamics (QED). On the other hand, it avoids the complications of a gauge theory as well as spin, chiral symmetry, etc. so it is fair to say that its primary purpose is to serve as a 'playground' on which to develop the necessary techniques of dealing with the strong coupling problem. Indeed, it is for this reason that, even after more than 40 years since Wick and Cutkosky first used the model to look for the relativistic bound state in the ladder approximation, it retains its popularity [17 - 23]. The generalization of the variational method to a realistic theory, namely QED, will be presented in a forthcoming publication [24] (for a preliminary account see [25]).

The Wick - Cutkosky Lagrangian in Euclidean space is given by

$$\mathcal{L} = \frac{1}{2}(\partial_\mu \Phi)^2 + \frac{1}{2}M_0^2 \Phi^2 + \frac{1}{2}(\partial_\mu \phi)^2 + \frac{1}{2}m^2 \phi^2 - g\Phi^2 \phi \quad (1.1)$$

where  $M_0$  is the bare mass of the heavy particle  $\Phi$ ,  $m$  is the mass of the light particle  $\phi$  and  $g$  is the coupling constant. As in (I) - (IV), we work in the quenched approximation of the theory and shall concentrate on those Green functions which involve one heavy particle interacting with an

arbitrary number of light particles. The generating functional for these Green functions is obtained after integration over the light degrees of freedom and is given by (see (I) and (II) for details)

$$Z[j, x] \propto \int_0^\infty d\beta \exp\left(-\frac{\beta}{2}M_0^2\right) \int_{x(0)=0}^{x(\beta)=x} \mathcal{D}x(t) \exp\{-S_{\text{eff}}[x(t)] - S_2[x(t), j]\} \quad . \quad (1.2)$$

Here the effective action

$$S_{\text{eff}} = \int_0^\beta dt \frac{1}{2}\dot{x}^2(t) - \frac{g^2}{2} \int_0^\beta dt_1 \int_0^\beta dt_2 \int \frac{d^4q}{(2\pi)^4} \frac{1}{q^2 + m^2} e^{iq \cdot (x(t_1) - x(t_2))} \quad (1.3)$$

is formulated in terms of the heavy particle trajectories parameterized by the proper time  $t$ . The meson source term

$$S_2[x(t), j] = -g \int d^4y j(y) \int_0^\beta dt \int \frac{d^4q}{(2\pi)^4} \frac{e^{iq \cdot (y - x(t))}}{q^2 + m^2} \quad (1.4)$$

produces  $n$  external mesons upon differentiation of  $Z[j, x]$  with respect to the meson source  $j(y)$  and setting  $j(y) = 0$ .

The variational method due to Feynman is based on the construction of a suitable trial action  $S_t$  containing variational parameters and on Jensen's inequality (or stationarity for complex actions)

$$\langle e^{-\Delta S} \rangle_{S_t} \stackrel{\text{stat}}{\simeq} e^{-\langle \Delta S \rangle_{S_t}} \quad , \quad (1.5)$$

where

$$\Delta S = S_{\text{eff}} - S_t \quad (1.6)$$

and the averaging is done with the weight function  $e^{-S_t}$ . This averaging must be done exactly and therefore the trial action can depend at most quadratically on the function  $x(t)$ .

Several remarks are in order here. First of all, one may wonder in what way a quadratic trial action could in any way be a reasonable approximation to the effective action in Eq. (1.3) which, after all, is exponential in  $x(t)$ . The important feature of  $S_{\text{eff}}$  (which, by construction, is shared by the trial action  $S_t$ ) is that it is non-local in the proper time  $t$ : For an 'average' path  $x(t)$  the separation  $x(t_1) - x(t_2)$  tends to be correlated with the proper time difference  $t_1 - t_2$  and so an unrestrained increase due to a quadratic term  $[x(t_1) - x(t_2)]^2$  in the trial action may be compensated for by a 'retardation function' in  $t_1 - t_2$ . Secondly, it is important to note that the approximation in Eq. (1.5) is a correctable one: if one so desires one can calculate arbitrarily precise corrections to the variational result by adding appropriate powers of  $\Delta S$  on the right hand side of this equation.

Another important feature of Eq. (1.5) is that it is easy to ensure that it reproduces the one loop perturbative result for *any* trial action whatsoever (see Ref. (I)). It goes without saying, however, that the more of the physics the trial action contains, the closer the numerical results of the 'leading order' result in Eq. (1.5) should be to the true situation. In particular, in the present paper we shall examine meson-'nucleon' scattering near threshold (for simplicity, we refer to the heavier particle as the 'nucleon' and the lighter as the meson). One expects large distance (time) effects to be important at threshold since the particles move very slowly relative to each other, but, on the other hand, short distance effects also remain relevant because of the normal divergences of the relativistic field theory. In other words, particle scattering near threshold is one situation where it is important that the trial action contains information about both the infrared and the ultraviolet behaviour of the

theory (another application where this would be important is in a confining theory like Quantum Chromodynamics; see [26]). In the variational approach under discussion it is once again the non-locality in the proper time which allows one to incorporate the physics of both these regimes into the trial action simultaneously through suitable behaviour of the retardation function for small and large values of  $t_1 - t_2$ .

It is the purpose of the present paper to examine to what extent this can be done for scattering, both analytically and numerically. A precursor to this work may be found in Ref. (III). There scattering was discussed at *zeroth* order in the variational approximation (i.e.  $S_{\text{eff}}$  was just replaced by  $S_t$ ). Although a drastic approximation, resulting in a Gaussian dependence on all external momenta, the information contained in the zeroth order variational scattering amplitude was already considerable: for example, the forward scattering amplitude had an analytic structure which contained the cuts associated with the production of an arbitrary number of mesons in the intermediate state. In fact, this is another general feature of this variational method: the untruncated Green functions explicitly contain parts of *all* Feynman diagrams and their associated analytic structure of any order in the coupling constant (see (IV)). Furthermore, it is possible to perform the non-perturbative truncation of this Green function analytically, yielding a rather concise formula for Green functions involving an arbitrary number of external mesons. In that paper, the vertex function of the theory ( $n = 1$ ) was examined in detail and it was found that there are large non-perturbative effects, particularly near the pair production threshold. In the present paper we generalize the variational *ansatz* for the trial action further without modifying the variational equations for the on-shell particles. Thus the vertex function remains unchanged but the variational scattering amplitude ( $n = 2$ ) gets more freedom to approximate the true off-shell propagation.

As in (III), we shall again pay particular attention to the question of unitarity near the lowest threshold of the forward scattering amplitude. Because unitarity is not automatic in the formalism, it serves as a useful guide to its success. At zeroth order, unitarity is already satisfied to within a factor of two. We shall find that, as expected, this is improved in the present calculation (i.e. at ‘first order’ in the variational calculation). Guides such as this are particularly important for the theory under consideration as the Wick-Cutkosky model does not have a strong coupling limit [27, 11] and so it is difficult to assess the quality of the variational calculation in the regime in which perturbation theory fails <sup>1</sup>.

This paper is organized in the following manner. In the next Section we describe the variational approach. In Section 3 we give the result for the general  $(2 + n)$ -point function. We use this result in Section 4 to derive the scattering amplitude for two external mesons (i.e.  $n = 2$ ) as a general function of the Mandelstam variables  $s$ ,  $t$  and  $u$  and examine its general structure as well as its region of convergence. In Section 5 we specialize to the s-channel near the first threshold and perform the necessary analytic continuation. Furthermore, we derive here important analytical results for the imaginary part of the scattering amplitude near threshold and in Section 6 we numerically investigate the question of unitarity. Finally, in Section 7 we conclude.

---

<sup>1</sup>This should not be taken to mean that there are no interesting non-perturbative effects even at modest couplings – the qualitative and quantitative differences between the perturbative and variational form factors near threshold observed in (IV) are but one of these.

## 2. The Variational Approach

The most general solvable trial action is of the form

$$S_t[x] = \int_0^\beta dt \frac{1}{2} \dot{x}^2 + \int_0^\beta dt_1 \int_0^\beta dt_2 f(t_1 - t_2) [x(t_1) - x(t_2)]^2 \quad , \quad (2.1)$$

where  $f(t_1 - t_2)$  can be thought off as a ‘retardation function’ depending on the proper time lapse  $t_1 - t_2$  between emission and re-absorption of mesons by the nucleon.

In actual calculations it is preferable to work in Fourier space and write the trial action in the form

$$S_t[b] = \sum_{k=0}^{\infty} A_k b_k^2 \quad (2.2)$$

where the  $b_k$  are the Fourier components of the nucleon path

$$x(t) = x \frac{t}{\beta} + \sum_{k=1}^{\infty} \frac{2\sqrt{\beta}}{k\pi} b_k \sin\left(\frac{k\pi t}{\beta}\right) \quad . \quad (2.3)$$

Defining  $b_0 = x/\sqrt{2\beta}$ , the free action is simply  $S_0 = \sum_{k=0}^{\infty} b_k^2$  and the nucleon propagator is given by

$$\begin{aligned} G_2(x) &= \frac{1}{8\pi^2} \int_0^\infty d\beta \frac{1}{\beta^2} \exp\left(-\frac{\beta}{2} M_0^2 - \frac{x^2}{2\beta}\right) \int \mathcal{D}b e^{-S_{\text{eff}}} \\ &\geq \frac{1}{8\pi^2} \int_0^\infty d\beta \frac{1}{\beta^2} \exp\left(-\frac{\beta}{2} M_0^2 - \frac{x^2}{2\beta}\right) \exp(-\langle \Delta S \rangle_{S_t}) \frac{\int \mathcal{D}b e^{-S_t}}{\int \mathcal{D}b e^{-S_0}} \end{aligned} \quad (2.4)$$

It is well known that near the pole it is the Fourier transform of  $G_2(x)$  which has a simple form. For this reason it is advantageous to apply the variational principle directly to  $G_2(p) = \int d^4x \exp(ip \cdot x) G_2(x)$  rather than to  $G_2(x)$  using a trial action which is also a function of  $p \cdot x$ . In (I) a simple trial action was constructed for the propagator by allowing an additional variational parameter  $\lambda$  which can be thought off as a rescaling of the momentum  $p$  or a ‘velocity’ parameter. The form used was

$$\tilde{S}_t = S_t - i\lambda p \cdot x \quad (2.5)$$

It was shown in (I) that in order to recover the correct pole behaviour of the propagator the proper time  $\beta$  must tend to infinity. In this limit all discrete sums over the Fourier modes  $A_k$  turn into integrals over the profile function  $A(E = k\pi/\beta)$ . The ‘profile function’  $A(E)$  is linked to the retardation function  $f(\sigma)$  through

$$A(E) = 1 + \frac{8}{E^2} \int_0^\infty d\sigma f(\sigma) \sin^2 \frac{E\sigma}{2} \quad . \quad (2.6)$$

The functional form of the retardation function,  $f(t_1 - t_2)$ , may be left free and is best determined using the variational principle. In practice, however, it is more convenient to use a particular parameterization containing a few variational parameters rather than a variational functional. This allows one to obtain analytic rather than numerical results. In our present numerical scheme it is also necessary for performing the analytic continuation from Euclidean time (where the variational calculation is done) to Minkowski time (where the scattering amplitude is evaluated). For the nucleon propagator it was found in (II) that it was quite sufficient to use trial actions which have a similar behaviour to the true action for small time intervals. For scattering, especially near particle production thresholds,

we also need the correct infrared behaviour of the theory. A particular example of a quantity which is sensitive to large distance scales is the imaginary part of a forward scattering amplitude near a threshold. It must rise linearly with momentum because of the limited phase space available to the total cross section which corresponds to it via the optical theorem. In Ref. (III) we used progressively more refined profile functions in order to investigate this. It was indeed found that whether or not the variational forward amplitude exhibited this linear rise (at zeroth order) was critically dependent on the infrared behaviour of the associated trial action. The variational principle came to our aid by providing the best form for the retardation function for all values of  $\sigma$  and therefore we could determine what the small as well as the large  $\sigma$  behaviour of  $f(\sigma)$  should be. In (III) it was shown that one can incorporate the correct large- and small- $\sigma$  behaviour by using the following functional form for the retardation function ('extended' parameterization):

$$f(\sigma) = \frac{C_1}{\sigma^2} [e^{-w_1\sigma} - C_2\sqrt{\sigma}e^{-w_2\sigma}] \quad , \quad (2.7)$$

with the requirement that  $w_1 > w_2$  and  $C_2 > 0$ . The associated profile function is

$$A(E) = 1 + \frac{2C_1}{E^2} \left[ E \arctan \frac{E}{w_1} - w_1 \ln \left( 1 + \frac{E^2}{w_1^2} \right) - 4C_2\sqrt{\pi} \left( \sqrt{\frac{1}{2} \left( \sqrt{w_2^2 + E^2} + w_2 \right)} - \sqrt{w_2} \right) \right] \quad (2.8)$$

having branch points at  $E = iw_2$  and  $E = iw_1$ . The variational parameters  $C_1, C_2, w_1$  and  $w_2$  were determined from the variational equations for the 2-point function  $G_2(p)$  with the trial action of Eq. (2.5) following the procedure described in (I) and (II).

### 3. The $(2 + n)$ point function

The  $(2 + n)$ -point function can be derived in a similar way to the propagator  $G_2(p)$ . In (IV) it was shown that the variational expression for the  $(2 + n)$  function is given by

$$G_{2,n}(p, p'; \{q\}) \propto \int_0^\infty d\beta \left[ \prod_{i=1}^n g \int_0^\beta d\tau_i \right] \exp \left[ -\frac{\beta}{2} M_0^2 \right] e^{-\langle \Delta \tilde{S} \rangle_{\tilde{s}_i}} \int d^4x \int \mathcal{D}x e^{-\tilde{S}_i[x(t)]} . \quad (3.1)$$

In terms of the Fourier components  $b_k$  the effective action in momentum space is

$$\tilde{S} = S[x(t)] + i \left[ \sqrt{\frac{2}{\beta}} b_0 \cdot \sum_{i=1}^{n+1} \alpha_i p_i - \sum_{k=1}^{\infty} Q_k^{(n)} \cdot b_k \right] \quad (3.2)$$

where

$$Q_k^{(n)} = \frac{2\sqrt{\beta}}{\pi k} \sum_{i=1}^n \sin \left( \frac{k\pi\tau_i}{\beta} \right) q_i \quad , \quad (3.3)$$

These additional terms on the right hand side (or, rather, their exponential) are just the plane waves appropriate for the  $n$  external mesons. The Euclidean momenta and the integration variables  $\alpha_i$  are defined in Fig. 1. <sup>2</sup>

---

<sup>2</sup> The unrestricted integration over all  $\tau_i$  in Eq. (3.1) may be replaced by an integration over  $\tau_i$  as indicated in Fig. 1, provided that all permutations of the meson momenta are summed over. In this way *one* wordline expression contains *many* different Feynman diagrams

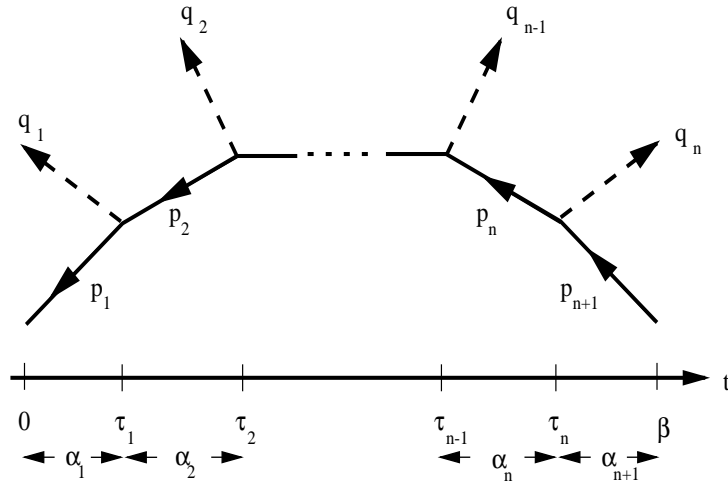


Figure 1: The definition of the relative times and momenta. Note that  $\tau_0 = 0$ ,  $\tau_{n+1} = \beta$ ,  $p_1 = -p$  and  $p_{n+1} = p'$ .

Given a true action of the above form, it was a natural choice in (IV) to take the trial action for the  $n$ -point function to be of the form

$$\tilde{S}_t = S_t + i \left[ \sqrt{\frac{2}{\beta}} \lambda A_0 b_0 \cdot \sum_{i=1}^{n+1} \alpha_i p_i - \sum_{k=1}^{\infty} \lambda A_k Q_k^{(n)} \cdot b_k \right] , \quad (3.4)$$

where  $\lambda$  and  $A_k$  are variational parameters which turned out to have the same variational equations independently of the number of external mesons  $n$ .<sup>3</sup>

Actually, one can do somewhat better than this without much effort and, indeed, it turns out to be physically sensible to choose a somewhat more general trial action than Eq. (3.4). The reason is the following: although we only consider on-shell Green functions, the intermediate nucleon lines in Fig. 1 are in general still off-shell. Therefore it might be useful to associate a different  $\lambda$  with each of the  $(n + 1)$  nucleon momenta in this action, thus allowing the trial action additional freedom to adjust itself to the fact that these internal lines have different virtualities. As we shall see, for the correct position of particle production thresholds in the intermediate state this choice of trial action will prove to be useful.

In the following, we briefly summarize the relevant results for a trial action of this form. The discussion follows (IV) closely, where the interested reader may find further details. Crucially, as we shall see shortly, the variational equation for the  $\lambda$ 's associated with the external legs reduce to the same equation as one found for the nucleon propagator, resulting in the same mass renormalization as before. Therefore, a consistent truncation of the Green function remains possible.

In short, the trial action which we shall use is given by

$$\tilde{S}_t = S_t + i \left[ \sqrt{\frac{2}{\beta}} A_0 b_0 \cdot \sum_{i=1}^{n+1} \alpha_i p_i \lambda_i - \sum_{k=1}^{\infty} A_k \tilde{Q}_k^{(n)} \cdot b_k \right] , \quad (3.5)$$

<sup>3</sup>The reason why the combination  $\lambda A_k$  appears in the last term of Eq. (3.4) is connected to the truncation of the Green function – see Ref. (IV).

where

$$\tilde{Q}_k^{(n)} = \frac{2\sqrt{\beta}}{\pi k} \sum_{i=1}^n \sin\left(\frac{k\pi\tau_i}{\beta}\right) (\lambda_{i+1}p_{i+1} - \lambda_i p_i) \quad , \quad (3.6)$$

and  $S_t$  is given by Eq. (2.2). Note that in the limit in which the coupling goes to zero the true action  $\tilde{S}$  becomes

$$\tilde{S}_0 = S_0 + i \left[ \sqrt{\frac{2}{\beta}} b_0 \cdot \sum_{i=1}^{n+1} \alpha_i p_i - \sum_{k=1}^{\infty} Q_k^{(n)} \cdot b_k \right] \quad , \quad (3.7)$$

so that  $A_k$  and  $\lambda_i$  must go to 1 in this limit. Writing the true action as

$$\tilde{S} = \tilde{S}_0 + S_1 \quad (3.8)$$

one obtains for the path integral of the exponential of the trial action, up to irrelevant overall constants,

$$\int \mathcal{D}\tilde{x} e^{-\tilde{S}_t} = \left[ \prod_{k=0}^{\infty} \frac{1}{A_k^2} \right] \exp \left\{ -\frac{1}{2\beta} \left[ A_0 \tilde{P}^2 + \frac{\beta}{2} \sum_{k=1}^{\infty} A_k \tilde{Q}_k^{(n)^2} \right] \right\} \quad . \quad (3.9)$$

where

$$\int \mathcal{D}\tilde{x} = \int d^4x \int_{x(0)=0}^{x(\beta)=x} \mathcal{D}x \quad . \quad (3.10)$$

Further, as part of  $\langle \Delta S \rangle$  we need

$$\langle \tilde{S}_0 - \tilde{S}_t \rangle_{\tilde{S}_t} = \frac{P \cdot \tilde{P}}{\beta} - \frac{\tilde{P}^2}{2\beta} (1 + A_0) + 2 \sum_{k=0}^{\infty} \left( \frac{1}{A_k} - 1 \right) - \sum_{k=1}^{\infty} \frac{\tilde{Q}_k^{(n)^2}{4} (1 + A_k) + \sum_{k=1}^{\infty} \frac{\tilde{Q}_k^{(n)} \cdot Q_k^{(n)}}{2} \quad , \quad (3.11)$$

For brevity we have defined the quantity  $P$  to be sum over all the nucleon lines' momenta weighted by the respective proper time intervals, i.e.

$$P = \sum_{i=1}^{n+1} \alpha_i p_i \quad . \quad (3.12)$$

$\tilde{P}$  is the equivalent quantity containing the relevant factors of  $\lambda_i$ , namely

$$\tilde{P} = \sum_{i=1}^{n+1} \alpha_i p_i \lambda_i \quad . \quad (3.13)$$

Combining these terms we obtain

$$\exp \left[ -\langle \tilde{S}_0 - \tilde{S}_t \rangle_{\tilde{S}_t} \right] \int \mathcal{D}\tilde{x} e^{-\tilde{S}_t} = \exp \left[ 2 \sum_{k=0}^{\infty} \left( 1 - \frac{1}{A_k} - \log A_k \right) + \sum_{i=1}^{n+1} \alpha_i p_i^2 \frac{\lambda_i (\lambda_i - 2)}{2} \right] \quad . \quad (3.14)$$

Finally, the weighted average of the interacting part of the action is given by

$$\langle S_1 \rangle_{\tilde{S}_t} = -\frac{g^2}{16\pi^2} \int_0^\beta dt_1 dt_2 \frac{1}{\tilde{\mu}^2(\sigma, T)} \int_0^1 dx_1 e \left( m\tilde{\mu}(\sigma, T), \frac{-i\tilde{W}^{(n)}}{\tilde{\mu}(\sigma, T)}, x_1 \right) \quad (3.15)$$

where  $e(x, y, z)$  is defined to be the exponential

$$e(x, y, z) = \exp \left( -\frac{x^2}{2} \frac{1-z}{z} - \frac{y^2}{2} z \right) \quad . \quad (3.16)$$

The quantity  $\tilde{\mu}^2(\sigma, T)$  appearing in the above equations is defined in terms of the ‘pseudotime’  $\mu^2(\sigma, T)$ , i.e.

$$\begin{aligned}\tilde{\mu}^2(\sigma, T) &= \frac{\sigma^2}{A_0\beta} + \mu^2(\sigma, T) \\ &= \frac{\sigma^2}{A_0\beta} + \frac{8\beta}{\pi^2} \sum_{k=1}^{\infty} \frac{1}{A_k k^2} \cos^2\left(\frac{k\pi T}{\beta}\right) \sin^2\left(\frac{k\pi\sigma}{2\beta}\right).\end{aligned}\quad (3.17)$$

Here we have introduced the relative and total times  $\sigma = t_1 - t_2$  and  $T = (t_1 + t_2)/2$  and the pseudotime  $\mu^2$ , after taking the  $\beta \rightarrow \infty$  limit, becomes

$$\mu^2(\sigma) = \frac{4}{\pi} \int_0^{\infty} dE \frac{1}{A(E)} \frac{\sin^2(E\sigma/2)}{E^2}.\quad (3.18)$$

The analytic structure as well as the asymptotic behaviour of the pseudotime in Eq. (3.18) is of great importance. This analytic structure is closely linked to the analytic structure of the profile function. In particular, parameterizations of the profile function which exhibit the same ultraviolet behaviour as the true action lead to a pseudotime  $\mu^2(\sigma)$  which grows linearly with  $\sigma$  for both  $\sigma \rightarrow 0$  and  $\sigma \rightarrow \infty$  and does not have poles or cuts in the half-plane where  $\mathcal{R}e(\sigma)$  is positive (see III).

The quantity  $\tilde{W}^{(n)}$  is defined by

$$\tilde{W}^{(n)} = \frac{\sigma}{\beta} \tilde{P} - \frac{2\sqrt{\beta}}{\pi} \sum_{k=1}^{\infty} \tilde{Q}_k^{(n)} \frac{1}{k} \cos\left(\frac{k\pi T}{\beta}\right) \sin\left(\frac{k\pi\sigma}{2\beta}\right).\quad (3.19)$$

It is equal to

$$\tilde{W}^{(n)} = \frac{\sigma}{2} (\lambda_1 p_1 + \lambda_{n+1} p_{n+1}) + \frac{1}{2} \sum_{i=1}^n (|\tau_i - t_1| - |\tau_i - t_2|) (\lambda_{i+1} p_{i+1} - \lambda_i p_i)\quad (3.20)$$

which simplifies to

$$\begin{aligned}\tilde{W}^{(n)} &= \text{sign}(\sigma) \left\{ \left[ \tau_{b+1} - \min(t_1, t_2) \right] \lambda_{b+1} p_{b+1} \right. \\ &\quad \left. + \sum_{i=b+2}^{a-1} \alpha_i \lambda_i p_i + \left[ \max(t_1, t_2) - \tau_{a-1} \right] \lambda_a p_a \right\} \quad a > b + 1 \\ &= \sigma \lambda_a p_a \quad a = b + 1.\end{aligned}\quad (3.21)$$

For the case  $a = b + 2$ , the sum appearing in Eq. (3.21) is defined to be empty. In other words,  $\tilde{W}^{(n)}$  is equal (up to a sign, which is not relevant as only the square of  $\tilde{W}^{(n)}$  enters) to the integral of the proper time multiplied by the modified nucleon’s four-momentum  $\lambda p$  for the duration of the exchange of the internal meson. Particular cases of interest, for the purpose of the eventual truncation of the Green function, are those where  $t_{1,2}$  are both smaller or both larger than all  $\tau_i$ , in which case  $\tilde{W}^{(n)} = \sigma \lambda_1 p_1$  and  $\sigma \lambda_{n+1} p_{n+1}$ , respectively.

Having calculated the above averages, one can now write down the expression for the (untruncated)  $(2 + n)$ -point function to first order in the variational framework

$$\begin{aligned}G_{2,n}(p, p'; \{q\}) &= \frac{N_0}{2g} \sum_{\mathcal{P}\{q_i\}} \left\{ \prod_{i=1}^{n+1} g \int_0^{\infty} d\alpha_i \exp \left[ -\frac{\alpha_i}{2} \left( M_0^2 + 2\Omega + p_i^2 [1 - (1 - \lambda_i)^2] \right) \right] \right\} \\ &\quad \cdot \exp \left[ \frac{g^2}{8\pi^2} \int_0^{\beta} dt_1 \int_0^{t_1} dt_2 \frac{1}{\mu^2(\sigma)} \int_0^1 dx_1 e \left( m\mu(\sigma), \frac{-i\tilde{W}^{(n)}}{\mu(\sigma)}, x_1 \right) \right].\end{aligned}\quad (3.22)$$

Here  $N_0$  is defined to be

$$N_0 = \frac{1}{A(0)} \exp\left(1 - \frac{1}{A(0)}\right). \quad (3.23)$$

For  $i = 1$  and  $i = n + 1$  we get the same on-shell relation between the bare mass and the renormalized mass as before, e.g. for  $i = 1$

$$M_0^2 + 2\Omega = M^2[1 - (1 - \lambda_1)^2] + \frac{g^2}{4\pi^2} \int_0^\infty \frac{d\sigma}{\mu^2(\sigma)} \int_0^1 dx_1 e\left(m\mu(\sigma), \frac{\lambda_1\sigma M}{\mu(\sigma)}, x_1\right) \quad (3.24)$$

where the quantity  $\Omega$  has been defined in Ref. (I). Further, we get the same variational equations for these two lambda's as before and so we write

$$\lambda_1 = \lambda_{n+1} = \lambda \quad (3.25)$$

The truncated  $(2 + n)$ -point function  $G_{2,n}^{tr}(p, p'; \{q\})$ , valid for on-shell external nucleon momenta, now reads

$$\begin{aligned} G_{2,n}^{tr}(p, p'; \{q\}) &= \frac{2g}{N_0} \sum_{\mathcal{P}\{q_i\}} \left\{ \prod_{i=2}^n g \int_0^\infty d\alpha_i \exp\left[-\frac{\alpha_i}{2} \left(M^2(1 - (1 - \lambda)^2) + p_i^2(1 - (1 - \lambda_i)^2)\right)\right] \right\} \\ &\quad \cdot \exp\left\{ -\frac{g^2}{8\pi^2} \int_0^1 du \left[ \int_0^\infty \frac{d\sigma}{\mu^2(\sigma)} \sum_{i=2}^n \alpha_i e\left(m\mu(\sigma), \frac{\lambda\sigma M}{\mu(\sigma)}, u\right) \right. \right. \\ &\quad \left. \left. - \int \frac{dt_1 dt_2}{\mu^2(\sigma)} e\left(m\mu(\sigma), \frac{-i\tilde{W}^{(n)}}{\mu(\sigma)}, u\right) \right] \right\}. \quad (3.26) \end{aligned}$$

where  $\mathcal{P}\{q_i\}$  denotes all possible permutations of  $q_i$ . Eq. (3.26) is the main result of this section.

## 4. The (2+2) scattering amplitude

In this section we focus our attention to the description of the scattering amplitude for meson-nucleon scattering. From the last equation of the previous section, substituting  $n = 2$ , we immediately obtain

$$\begin{aligned} G_{2,2}(p, q_1, q_2) &= \frac{2g^2}{N_0} \sum_{\mathcal{P}\{q_1, q_2\}} \int_0^\infty d\alpha_2 \exp\left\{-\frac{\alpha_2}{2} \left[M^2(1 - (1 - \lambda)^2) + p_2^2(1 - (1 - \lambda_2)^2)\right] \right. \\ &\quad \left. + \frac{g^2}{8\pi^2} \tilde{\Xi}(p, q_1, q_2; \alpha_2)\right\}. \quad (4.1) \end{aligned}$$

The function  $\tilde{\Xi}$  is defined as

$$\begin{aligned} \tilde{\Xi}(p, q_1, q_2; \alpha_2) &= \int_0^1 dx_1 \left\{ \int \frac{dt_1 dt_2}{\mu^2(\sigma)} e\left(m\mu(\sigma), \frac{-i\tilde{W}^{(2)}}{\mu(\sigma)}, x_1\right) \right. \\ &\quad \left. - \int_0^\infty \frac{d\sigma}{\mu^2(\sigma)} \alpha_2 e\left(m\mu(\sigma), \frac{\lambda\sigma M}{\mu(\sigma)}, x_1\right) \right\}. \quad (4.2) \end{aligned}$$

The  $t_1 - t_2$  integration region in Eq. (4.2) is shown in Fig. 2. Depending on the ordering of the internal meson's emission and absorption times  $t_2$  and  $t_1$  with respect to the proper times at which

the external mesons interact with the nucleon, i.e.  $\tau_1$  and  $\tau_2$ , the function  $\tilde{W}^{(2)}$  assumes a different value. Explicitly,

$$\begin{aligned}
\tilde{W}^{(2)} &= (\tau_1 - t_2)\lambda p_1 + (t_1 - \tau_1)\lambda_2 p_2 && t_2 < \tau_1, \tau_1 < t_1 < \tau_2 \\
&= (t_1 - t_2)\lambda_2 p_2 && \tau_1 < t_1, t_2 < \tau_2 \\
&= (\tau_2 - t_2)\lambda_2 p_2 + (t_1 - \tau_2)\lambda p_3 && \tau_1 < t_2 < \tau_2, \tau_2 < t_1 \\
&= (\tau_1 - t_2)\lambda p_1 + \alpha_2 \lambda_2 p_2 + (t_1 - \tau_2)\lambda p_3 && t_2 < \tau_1, \tau_2 < t_1.
\end{aligned} \tag{4.3}$$

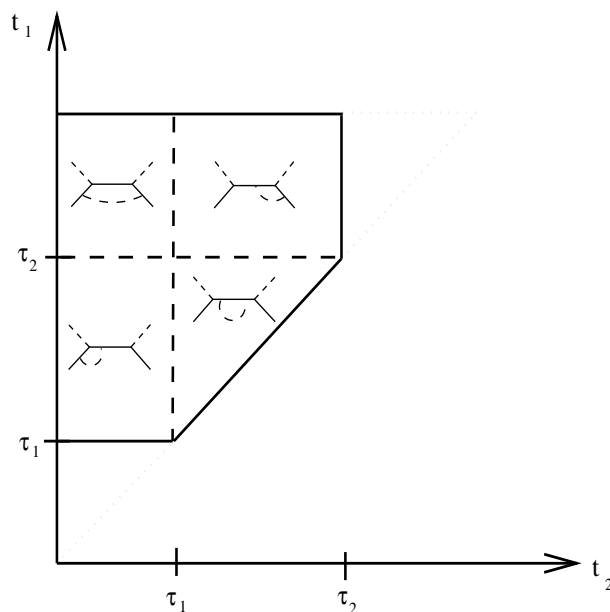


Figure 2: The  $(t_1 - t_2)$  - integration region is shown enclosed by the solid line. The (dotted) triangular regions are those relevant to the dressing of the external legs and have been removed in the truncated amplitude. Also shown are the relevant diagrammatic representations (for the direct diagram) of the *action* in the particle representation

Although the integration variable  $\alpha_2$  in the expression for the Green function in Eq. (3.26) is a time difference, the integration variables  $t_1$  and  $t_2$  in Eq. (4.2) are still absolute times. This leads to a spurious dependence of  $\tilde{W}^{(2)}$  and the integration limits of the  $(t_1 - t_2)$  - integration on the absolute times  $\tau_1$  and  $\tau_2$ <sup>4</sup>. In order to eliminate this spurious dependence it is convenient to make a transformation of the integration variables  $t_1$  and  $t_2$  to two variables which *are* expressed as time differences. Clearly  $\sigma = t_1 - t_2$  is a suitable choice for one of these. It is convenient to define the second variable  $x_2$  in a different way for each of the integration regions depicted in Fig. 2. We shall discuss each of these regions below.

Before proceeding, let us make the change to the Minkowski space Mandelstam variables  $s$ ,  $t$  and  $u$  (as well as Minkowski  $q^2$  and  $q'^2$  for the external mesons), which are defined in terms of the Euclidean

<sup>4</sup>It should be remembered that  $\tau_1$  and  $\alpha_3$  have already been integrated over in Eq. (3.26) in order to truncate the Green function, so a dependence on these variables in Eq. (3.26) would be non-sensical.

momenta  $p_1, p_3, q_1$  and  $q_2$  through

$$\begin{aligned} s &= -(p_1 + q_1)^2 \\ t &= -(p_1 - p_3)^2 \\ u &= -(p_1 + q_2)^2 \quad . \end{aligned} \quad (4.4)$$

In contrast to the usual formalism this change from Euclidean to Minkowski four-momenta is a trivial one in the worldline approach, as there are no four-momentum integrals left to be done in the expression for the Green function.

It is rather useful to break up the function  $\tilde{\Xi}$  not only into the components corresponding to the two vertex corrections, the propagator correction and the box diagram depicted in Fig. 2, i.e.

$$\tilde{\Xi}(s, t, q^2, q'^2; \alpha_2) = \tilde{\Xi}_V(s, q^2; \alpha_2) + \tilde{\Xi}_V(s, q'^2; \alpha_2) + \tilde{\Xi}_P(s; \alpha_2) + \tilde{\Xi}_B(s, t, q^2, q'^2; \alpha_2) \quad , \quad (4.5)$$

but also to immediately extract their leading  $\alpha_2$  - behaviour. The reason for this is that  $\alpha_2$  is the proper time conjugate to the intermediate nucleon's momentum and so one might intuitively expect that the large  $\alpha_2$  - behaviour is particularly important close to the threshold, i.e. close to where real particles could be produced in the intermediate state. This is analogous to what happens for the nucleon propagator itself – as indicated in Section 2, the on-shell propagator corresponds to letting  $\beta \rightarrow \infty$ . This physical interpretation associated with the use of the Fock–Schwinger proper time formalism makes it advantageous over the use of the usual Feynman parameters.

Explicitly, the component of  $\tilde{\Xi}$  corresponding to the bottom left hand integration region in Fig. 2 may be written as

$$\tilde{\Xi}_V(s, q^2; \alpha_2) = \Xi_V^0(s, q^2) + \Xi_V(s, q^2; \alpha_2) \quad , \quad (4.6)$$

where  $\Xi_V^0(s, q^2)$  does not depend on  $\alpha_2$  and  $\Xi_V(s, q^2; \alpha_2)$  goes to zero as  $\alpha_2 \rightarrow \infty$ . In these variables, the constant piece  $\Xi_V^0(s, q^2)$  for the direct diagram (we shall discuss the crossed diagram later) becomes

$$\Xi_V^0(s, q^2) = \int_0^1 dx_1 dx_2 \int_0^\infty d\sigma \frac{\sigma}{\mu^2(\sigma)} e\left(m\mu(\sigma), \frac{\sigma}{\mu(\sigma)} W_V(x_2), x_1\right) \quad . \quad (4.7)$$

Here the variable  $x_2$  is defined as the time interval  $\tau_1 - t_2$  between the external and internal meson's interaction time with the nucleon, scaled by  $\sigma$ , and  $W_V^2(x_2)$  is given by

$$W_V^2(x_2) = \left[ x_2 \lambda_2 + x_2^2 (\lambda - \lambda_2) \right] \lambda M^2 + \lambda_2 (1 - x_2) \left[ s (\lambda_2 + x_2 (\lambda - \lambda_2)) - \lambda x_2 q^2 \right] \quad . \quad (4.8)$$

On the other hand, the piece of  $\tilde{\Xi}_V$  which depends on  $\alpha_2$  is

$$\Xi_V(s, q^2; \alpha_2) = - \int_0^1 dx_1 dx_2 \int_0^\infty d\sigma \frac{\sigma}{\mu^2(\sigma + \alpha_2)} e\left(m\mu(\sigma + \alpha_2), \frac{(\sigma + \alpha_2)}{\mu(\sigma + \alpha_2)} W_V\left(\frac{\sigma}{\sigma + \alpha_2} x_2\right), x_1\right) \quad , \quad (4.9)$$

where  $\sigma$  has been shifted by  $\alpha_2$  and  $x_2$  has been rescaled accordingly. Also, it is easily seen that the expression for the second vertex (top right hand region in Fig. 2) is the same, except that  $q^2$  needs to be replaced by  $q'^2$ .

In a similar way to the vertex function discussed in (IV) the representations Eqs. (4.7) and (4.9) for  $\tilde{\Xi}_V(s, q^2; \alpha_2)$  and  $\tilde{\Xi}_V(s, q'^2; \alpha_2)$  do not necessarily converge for all  $s$ . In fact, if we restrict ourselves to the case where the external mesons are on-shell (i.e.  $q^2 = q'^2 = m^2$ ) then Eqs. (4.7) and (4.9) are



grows like  $\alpha_2$ , as may be seen in Fig. 2. Clearly this is the only region for which this happens. It is also no accident that the expression for  $\Xi_P^1$  looks very similar to those encountered in the discussion of the renormalization of the nucleon propagator in (I)

$$\Xi_P^1(s) = \int_0^1 dx_1 \int_0^\infty \frac{d\sigma}{\mu^2(\sigma)} \left\{ e\left(m\mu(\sigma), \frac{\sigma}{\mu(\sigma)}\lambda M, x_1\right) - e\left(m\mu(\sigma), \frac{\sigma}{\mu(\sigma)}\lambda_2\sqrt{s}, x_1\right) \right\} , \quad (4.11)$$

the only difference being that there it only applied to the on-shell propagator, while  $\Xi_P^1$  also contains off-shell information. Indeed, as was proven for the general  $n$ -point function in (IV), the variational calculation – if expanded in the coupling – reproduces perturbation theory to one loop order exactly, *including* the off-shell behaviour of the internal propagator.

The constant piece contributing to  $\tilde{\Xi}_P$  is given by

$$\Xi_P^0(s) = - \int_0^1 dx_1 \int_0^\infty d\sigma \frac{\sigma}{\mu^2(\sigma)} e\left(m\mu(\sigma), \frac{\sigma}{\mu(\sigma)}\lambda_2\sqrt{s}, x_1\right), \quad (4.12)$$

while the piece that vanishes as  $\alpha_2 \rightarrow \infty$  becomes, after shifting the  $\sigma$  integration by  $\alpha_2$  as before,

$$\Xi_P(s; \alpha_2) = \int_0^1 dx_1 \int_0^\infty d\sigma \frac{\sigma}{\mu^2(\sigma + \alpha_2)} e\left(m\mu(\sigma + \alpha_2), \frac{\sigma + \alpha_2}{\mu(\sigma + \alpha_2)}\lambda_2\sqrt{s}, x_1\right) . \quad (4.13)$$

Clearly, the region of convergence of the representation for  $\tilde{\Xi}_P$  (Eqs. (4.10–4.13)) is the same as that of  $\tilde{\Xi}_V$ , i.e.  $s > 0$ . Also, it is relevant to the subsequent discussion of the region of convergence of the  $\alpha_2$  - integration that in the  $s$  channel  $\Xi_P^1$  is positive.

Finally, the integration over the region where the action is represented by the box diagram is given by

$$\Xi_B(s, t, q^2, q'^2; \alpha_2) = \int_0^1 dx_1 dx_2 \int_0^\infty d\sigma \frac{\sigma}{\mu^2(\sigma + \alpha_2)} e\left(m\mu(\sigma + \alpha_2), \frac{\sigma + \alpha_2}{\mu(\sigma + \alpha_2)}W_B, x_1\right) , \quad (4.14)$$

where

$$W_B^2 = \frac{(\sigma\lambda + \alpha_2\lambda_2)}{(\sigma + \alpha_2)^2} (\sigma\lambda M^2 + \alpha_2\lambda_2 s) - \left(\frac{\sigma\lambda}{\sigma + \alpha_2}\right)^2 (1-x_2)x_2 t - \frac{\sigma\alpha_2\lambda\lambda_2}{(\sigma + \alpha_2)^2} [x_2 q^2 + (1-x_2)q'^2] . \quad (4.15)$$

This time there is not even a constant term in  $\alpha_2$ , and the representation converges (for on-shell external mesons) as long as  $t < 4M^2$ , i.e. in the  $u$  and  $s$  channel.

In short, the contribution to the scattering amplitude due to the direct diagram is given by

$$A_{2,2}^{\text{direct}}(s, t, u, q^2, q'^2) = \mathcal{F}(s, q^2, q'^2) \int_0^\infty d\alpha_2 \exp \left\{ \frac{\alpha_2}{2} [1 - (1 - \lambda_2)^2] [s - \tilde{s}(s)] + \frac{g^2}{8\pi^2} \Xi(s, t, q^2, q'^2; \alpha_2) \right\} , \quad (4.16)$$

where

$$\tilde{s}(s) = \frac{1}{1 - (1 - \lambda_2)^2} \left[ (1 - (1 - \lambda)^2)M^2 + \frac{g^2}{4\pi^2} \Xi_P^1(s) \right] \quad (4.17)$$

and

$$\mathcal{F}(s, q^2, q'^2) = \frac{2g^2 N_1}{\lambda} \exp \left[ \frac{g^2}{8\pi^2} \left( \Xi_V^0(s, q^2) + \Xi_V^0(s, q'^2) + \Xi_P^0(s) \right) \right] . \quad (4.18)$$

Furthermore  $N_1 = \lambda Z/N_0$  where  $Z$  is the residue at the pole of the propagator. Note that for reasonably small couplings  $\tilde{s}$  is ‘close’ to  $M^2$  and that for  $s > M^2$  it is larger than  $M^2$ .

Let us now come back to the question of the analytic structure of this amplitude. It is clear from Eq. (4.16) that not only does one need to address the convergence criteria of the  $\sigma$  - integration, but also simultaneously those of the  $\alpha_2$  integration. It is for this reason that the analytic structure of the scattering amplitude is much richer than that of the vertex function in (IV). It is clear from Eq. (4.16) that for the  $\alpha_2$  - integration to converge we require  $s < \tilde{s}$  (note that  $\lambda$  is always less than 1). However,  $\tilde{s}$ , using the representation for  $\Xi_P^1$  in Eq. (4.11), is only defined for  $s > 0$ . So at the moment our Green function is only defined in a region  $0 < s < \tilde{s}$  and  $t < 4M^2$ , i.e. except for a limited region of the  $u$  - channel (Fig. 3) it is only defined outside the three physical regions for the process. Importantly, however, for the analytic continuation there *does* exist a region where it is defined. Because of the complicated interplay between the convergence of the  $\sigma$  - and  $\alpha_2$  - integrations one needs to analytically continue the above representation on a case by case basis. In the present paper we are interested in doing this for the  $s$ -channel.

Before we proceed, let us write down the amplitude for the crossed channel. It is given by

$$A_{2,2}^{\text{crossed}}(s, t, u, q^2, q'^2) = A_{2,2}^{\text{direct}}(u, t, s, q'^2, q^2). \quad (4.19)$$

Hence, again for on-shell external mesons, the representations above are only appropriate for  $A_{2,2}^{\text{crossed}}$  in the region  $0 < u < \tilde{s}$  and  $t < 4M^2$ . As may be seen in Fig. 3, this includes some of the physical region of the  $s$  channel. Indeed, as we shall concentrate our attention on the region near the threshold at  $s = (M + m)^2$ , this representation of  $A_{2,2}^{\text{crossed}}$  suffices for our purposes.

## 5. Unitarity in the $s$ channel near threshold

In order to be able to describe scattering of on-shell mesons off the nucleon in the  $s$  channel, the convergence requirement of the  $\alpha_2$  - integration of the direct diagram requires the amplitude in Eq. (4.16) to be analytically continued so that it converges for  $s > \tilde{s}$ . This may be done in an analogous manner to a Wick rotation as in Refs. (III,IV): for  $s$  infinitesimally above the cut, i.e.  $s \rightarrow s + i\epsilon$ , one may deform the  $\alpha_2$  - integration in such a way that it runs along the positive imaginary axis. This is possible because the contribution of the quarter circle at infinity vanishes and because the analytic behaviour of the pseudotime  $\mu^2(\sigma)$  is known. Changing variables to  $\alpha_2 \rightarrow \alpha_2/i$ , and suppressing the dependence on  $q^2 = q'^2 = m^2$  for notational simplicity, one obtains

$$\begin{aligned} A_{2,2}^{\text{direct}}(s, t) &= i\mathcal{F}(s) \int_0^\infty d\alpha_2 \exp \left\{ i\frac{\alpha_2}{2} [1 - (1 - \lambda_2)^2] [s - \tilde{s}(s) + i\epsilon] + \frac{g^2}{8\pi^2} \Xi(s, t; i\alpha_2) \right\} \quad (5.1) \\ &= \frac{-2\mathcal{F}(s)}{[1 - (1 - \lambda_2)^2] [s - \tilde{s}(s) + i\epsilon]} + i\mathcal{F}(s) \int_0^\infty d\alpha_2 \exp \left\{ i\frac{\alpha_2}{2} [1 - (1 - \lambda_2)^2] [s - \tilde{s}(s)] \right\} \\ &\quad \cdot \left\{ \exp \left[ \frac{g^2}{8\pi^2} \Xi(s, t; i\alpha_2) \right] - 1 \right\}, \end{aligned}$$

where the latter expression, obtained by adding and subtraction a ‘modified Born term’, does not require an  $i\epsilon$  prescription for convergence and is therefore more suitable for numerical evaluation.

This expression for the amplitude converges in the region of interest. Together with the crossed diagram, which does not have to be analytically continued as long as one does not move more than about one nucleon mass away from the lowest threshold (and therefore remains real), it yields the complete scattering amplitude. Furthermore, it should be noted that for the special case of forward

scattering the expressions for  $\tilde{\Xi}$  naturally simplify somewhat. This is particularly true for the contribution of the box diagram to the action, where the  $x_2$  - integration may be carried out trivially when  $t = 0$  and  $q^2 = q'^2$ . Also, the two vertex contributions are, of course, identical whenever the latter of these conditions is fulfilled.

It is relatively straightforward to evaluate the crossed diagram numerically. Both the  $\alpha_2$  - as well as the  $\sigma$  - integral in  $\Xi(u, t; \alpha_2)$  converge exponentially, so simple Gaussian quadrature is quite adequate (we typically used 64, 72 or 96 Gaussian points per integration). The direct diagram, however is much more difficult to handle as in this case the integrands are oscillatory functions. In particular, the  $\alpha_2$  - integration only converges relatively slowly as  $\alpha_2 \rightarrow \infty$ . Moreover, the separate contributions to  $\Xi(s, t; \alpha_2)$  arising from the vertex, propagator and box diagrams oscillate with different frequencies for asymptotic  $\alpha_2$ , so that the numerical behaviour of the exponential of  $\Xi(s, t; \alpha_2)$  is rather erratic. This means that for a reasonably reliable result one needs to integrate up to rather large values of  $\alpha_2$ . We do this integral using the adaptive routine D01ASF for sine and cosine transforms from the NAG Fortran library.

We shall now turn to the question of the unitarity of the scattering amplitude near the lowest threshold. As mentioned in the Introduction, this is an interesting quantity to examine because one expects non-perturbative effects to be particularly strong at thresholds. Below the first inelastic threshold, unitarity implies that the total elastic cross section is related to the forward scattering amplitude. In the centre of mass system

$$\sigma_{\text{el}}(s) = \frac{1}{2|\mathbf{p}|\sqrt{s}} \text{Im} A(s, 0) \quad , \quad (5.2)$$

where  $\mathbf{p}$  is the centre of mass three-momentum and the elastic cross section is given by

$$\sigma_{\text{el}}(s) = \int d\Omega \frac{1}{64\pi^2 s} |A(s, t)|^2 \quad . \quad (5.3)$$

Near threshold the elastic scattering cross section is, of course, dominated by the real part of the amplitude because the imaginary part has to rise linearly with momentum from zero at threshold. This means that  $\sigma_{\text{el}}$  is not particularly sensitive to the exact position of the threshold. For the imaginary part of the forward scattering amplitude, however, the threshold position is of supreme importance. As was seen at zeroth order in (III), a linear rise with  $|\mathbf{p}|$  as well as a correct threshold position was not assured for an arbitrary trial action. In particular, the large- $\sigma$  behaviour of the retardation function entering this action was found to be crucial.

At first order one does not expect this to be quite as severe, as at least agreement with one-loop perturbation theory (which has the correct threshold behaviour) *is* assured for an arbitrary trial action. Nevertheless, the basic point remains the same: threshold behaviour is governed by the large distance behaviour of the action and therefore we expect some sensitivity to the large -  $\sigma$  behaviour of the retardation function. Hence it is advisable to spend some time examining the dependence of the imaginary part on the form of the profile function  $A(E)$ .

## 5.1 $\text{Im}A(s, 0)$ near Threshold

Before doing this, it is actually very instructive to have a look at  $\text{Im}A(s, 0)$  in perturbation theory. To leading order in  $|\mathbf{p}|$ , for each of the diagrams which includes a vertex correction, one obtains near

the threshold

$$\text{Im } A_V^{\text{pert.}}(s, 0) = -32\alpha^2\pi \frac{M^4}{(4M^2 - m^2)(M + m)m^2} |\mathbf{p}| + \mathcal{O}(\mathbf{p}^2) \quad , \quad (5.4)$$

the term involving the self energy of the intermediate propagator is

$$\text{Im } A_P^{\text{pert.}}(s, 0) = 32\alpha^2\pi \frac{M^4}{(2M + m)^2(M + m)m^2} |\mathbf{p}| + \mathcal{O}(\mathbf{p}^2) \quad , \quad (5.5)$$

and the box diagram yields

$$\text{Im } A_B^{\text{pert.}}(s, 0) = 32\alpha^2\pi \frac{M^4}{(2M - m)^2(M + m)m^2} |\mathbf{p}| + \mathcal{O}(\mathbf{p}^2) \quad . \quad (5.6)$$

Altogether, the leading contribution to the imaginary part is therefore given by

$$\text{Im } A^{\text{pert.}}(s, 0) = 128\alpha^2\pi \frac{M^4}{(4M^2 - m^2)^2(M + m)} |\mathbf{p}| + \mathcal{O}(\mathbf{p}^2) \quad . \quad (5.7)$$

Even though each diagram separately is divergent as the meson mass  $m$  goes to zero, this divergence cancels in the complete amplitude. For the physical value of  $\frac{m}{M} \approx \frac{1}{7}$  this means that the individual diagrams are something like 50 times as large as the final result. This makes the task of calculating the imaginary part of the variational expression for the forward scattering amplitude in Eq. (5.1) even more formidable than it already is – not only does one have the numerical problems mentioned above, one also should expect large cancelations between the various components of  $\Xi(s, t; \alpha_2)$ .

At first sight it may appear that the lowest threshold will open up as soon as  $s$  is large enough so that one needs to work with the complex representation in Eq. (5.1) rather than the purely real representation of Eq. (4.16), i.e.  $s > \tilde{s}(s)$ . Certainly, for  $0 < s < \tilde{s}(s)$  the amplitude must be real, because in this region Eq. (4.16) is valid. It is useful to examine the reason why Eq. (5.1), which is also valid in this region of  $s$ , does not develop an imaginary part here. To this end we shall define

$$\mathcal{D}(s) = \frac{1}{2} \left[ 1 - (1 - \lambda_2)^2 \right] [s - \tilde{s}(s)] \quad (5.8)$$

and

$$G(\alpha_2) = \exp \left\{ \frac{g^2}{8\pi^2} \Xi(s, t; i\alpha_2) \right\} - 1 \quad . \quad (5.9)$$

Hence the imaginary part of the forward scattering amplitude is related to

$$\int_0^\infty d\alpha_2 [\cos(\alpha_2 \mathcal{D}) \text{Re } G(\alpha_2) - \sin(\alpha_2 \mathcal{D}) \text{Im } G(\alpha_2)] \quad . \quad (5.10)$$

Using the facts that  $G(\alpha_2) = G^*(-\alpha_2)$ , that  $G(\alpha_2)$  has a cut along the positive imaginary axis and that it vanishes sufficiently fast as  $\alpha_2 \rightarrow \infty$ , one may easily prove, using dispersion methods, that

$$\int_0^\infty d\alpha_2 \cos(\alpha_2 \mathcal{D}) \text{Re } G(\alpha_2) = - \int_0^\infty d\alpha_2 \sin(\alpha_2 |\mathcal{D}|) \text{Im } G(\alpha_2) \quad . \quad (5.11)$$

Hence the two contributions to the imaginary part of the scattering amplitude in Eq. (5.10) cancel each other when  $\mathcal{D} < 0$ , i.e.  $s < \tilde{s}(s)$ , as required. For  $s > \tilde{s}(s)$  they remain identical in magnitude, but add. This is a useful property as it means that the amount of computer time required in the

numerical integrations involved in the calculation of the imaginary part of Eq. (5.1) is cut by a factor of 2.

Just because Eq. (5.1) *may* develop an imaginary part for  $s$  above  $\tilde{s}$  does not mean that it *will* do so. In fact, one may use a similar argument to that used in the investigation of the threshold position in (III) to show that the imaginary part only starts somewhat above  $\tilde{s}$ . Let us write  $\Xi(s, 0; \alpha_2)$  in Eq. (4.16) as a Laplace transform:

$$\frac{g^2}{8\pi^2} \Xi(s, 0; \alpha_2) \equiv \int_0^\infty dE \tilde{\rho}(E, s) e^{-E\alpha_2} . \quad (5.12)$$

Here  $\tilde{\rho}(E, s)$  is essentially the counterpart of the weight function  $\rho(E)$  encountered in the zeroth order calculation in (III). It was found, in fact, that  $\rho(E)$  is only non-zero for  $E$  larger than a critical value  $E_0$  and this will be also true for  $\tilde{\rho}$ , as will be shown below. Expanding the exponential in Eq. (4.16) with  $s \rightarrow s + i\epsilon$  and performing the  $\alpha_2$  - integration then yields

$$\mathcal{I}m A_{2,2}^{\text{direct}}(s, 0) = \pi \mathcal{F}(s) \sum_{n=1}^{\infty} \frac{1}{n!} \int_{E_0}^{\infty} dE_1 \dots dE_n \tilde{\rho}(E_1, s) \dots \tilde{\rho}(E_n, s) \delta\left(\sum_{i=1}^n E_i - \mathcal{D}(s)\right) \quad (5.13)$$

Only when the  $\delta$ -function is fulfilled an imaginary part develops. With this observation we proceed to obtain an analytic expression for the leading behavior of the imaginary part of the amplitude near threshold. Given the difficulties with the numerical evaluation of Eq. (5.1), in particular in view of the large cancelations expected between  $\Xi_V$ ,  $\Xi_P$  and  $\Xi_B$ , the possibility of having an analytic expression is indeed fortunate. The key to obtaining this threshold behaviour is the observation that below the first inelastic threshold only the  $n = 1$  term in Eq. (5.13) contributes. This amounts to expanding the exponential in the expression for the amplitude Eq. (4.16) and keeping only the first term; i.e.

$$\mathcal{I}m A_{2,2}^{\text{direct}}(s, 0) = \frac{g^2}{8\pi^2} \mathcal{F}(s) \mathcal{I}m \int_0^\infty d\alpha_2 e^{\alpha_2 \mathcal{D}(s)} \Xi(s, 0; \alpha_2) \quad E_0 < \mathcal{D}(s) < 2E_0 . \quad (5.14)$$

Below the first inelastic threshold the imaginary part of the forward amplitude is then simply given by

$$\mathcal{I}m A_{2,2}^{\text{direct}}(s, 0) = \mathcal{F}(s) \tilde{\rho}(\mathcal{D}(s), s) \Theta(\mathcal{D}(s) - E_0) \quad (5.15)$$

where we made use of the Laplace transform of  $\Xi$  defined in Eq. (5.12).

In practice, the weight function  $\tilde{\rho}(E, s)$  can be determined neither numerically (as inverse Laplace transforms are notoriously unstable) nor analytically because of the complicated  $\alpha_2$  - dependence of the function  $\Xi$ . The only case where the inverse Laplace transformation can be performed is near threshold which is known to be dominated by large values of  $\alpha_2$ . In this case we can approximate the pseudotime by its asymptotic behaviour

$$\mu^2(\alpha_2) \xrightarrow{\alpha_2 \rightarrow \infty} \frac{\alpha_2}{A(0)} + 4\xi(0) + \mathcal{O}(e^{-\alpha_2}) . \quad (5.16)$$

This allows us to evaluate the corresponding asymptotic expressions for the  $\Xi$ -functions. For example, the propagator diagram's contribution becomes

$$\begin{aligned} \Xi_P(\alpha_2) \rightarrow A(0) \int_0^\infty d\sigma \int_0^1 dx_1 \frac{\sigma}{\alpha_2 + \sigma + 4\xi(0)} \exp \left[ - \left( \frac{m^2}{2A(0)} \frac{1-x_1}{x_1} + \frac{A(0)}{2} \lambda_2^2 s x_1 \right) (\alpha_2 + \sigma) \right] \\ \cdot \exp \left[ -4A(0)\xi(0) \left( \frac{m^2}{2A(0)} \frac{1-x_1}{x_1} - \frac{A(0)}{2} \lambda_2^2 s x_1 \right) \right] . \quad (5.17) \end{aligned}$$

The above form is not a fully consistent expansion in inverse powers of  $1/\alpha_2$  since the exponential function will also contribute to such terms. Nevertheless it is a convenient form to perform the inverse Laplace transform as we may use (Ref. [28], Eq. (5.5.9))

$$\mathcal{L}^{-1}\left(\frac{e^{-a\alpha_2}}{\alpha_2 + b}; \alpha_2\right)(E) = e^{-b(E-a)} \Theta(E-a) \quad (5.18)$$

to obtain

$$\tilde{\rho}_P(E, s) \simeq \frac{g^2}{8\pi^2} \frac{A(0)}{E^2} \int_0^1 dx_1 \Theta(E - E_0(s, x_1)) \exp\left[-Q^2(s, x_1, E) \xi(0)\right]. \quad (5.19)$$

Here

$$E_0(s, x_1) = \frac{m^2}{2A(0)} \frac{1-x_1}{x_1} + \frac{A(0)}{2} \lambda_2^2 s x_1 \quad (5.20)$$

determines the minimal value of  $E$  (see below) and

$$Q^2(s, x_1, E) = 4A(0) \left[ \frac{m^2}{2A(0)} \frac{1-x_1}{x_1} - \frac{A(0)}{2} \lambda_2^2 s x_1 + E - E_0(s, x_1) \right] \quad (5.21)$$

is a kind of effective momentum transfer (one should remember from (III) that  $6\xi(0)$  is the mean square radius of the dressed particle in lowest variational order).

Similarly we obtain for the asymptotic form of  $\Xi$  in the box diagram

$$\begin{aligned} \Xi_B(\alpha_2) \rightarrow & A(0) \int_0^\infty d\sigma \int_0^1 dx_1 \frac{\sigma}{\alpha_2 + \sigma + 4\xi(0)} \exp\left[-E_0(s, x_1)\alpha_2 - Q^2(s, x_1, E_0) \xi(0)\right] \\ & \cdot \exp\left\{-\left[\frac{m^2}{2A(0)} \frac{1-x_1}{x_1} + \frac{A(0)x_1\lambda_2}{2} (\lambda(s + M^2 - m^2) - \lambda_2 s)\right] \sigma\right\} \end{aligned} \quad (5.22)$$

where again we have neglected terms of order  $1/\alpha_2$  in the argument of the exponential function. Using the formula (5.18) we get

$$\tilde{\rho}_B(E, s) \simeq \frac{g^2}{8\pi^2} \int_0^1 dx_1 \Theta(E - E_0(s, x_1)) \frac{A(0)}{E_1^2(s, x_1, E)} \exp\left[-Q^2(s, x_1, E) \xi(0)\right]. \quad (5.23)$$

where

$$E_1(s, x_1, E) = \frac{m^2}{2A(0)} \frac{1-x_1}{x_1} + \frac{A(0)x_1\lambda_2}{2} (\lambda(s + M^2 - m^2) - \lambda_2 s) + E - E_0(s, x_1). \quad (5.24)$$

Finally the  $\Xi$ -function in the vertex diagram has the asymptotic limit

$$\begin{aligned} \Xi_V(\alpha_2) \rightarrow & -A(0) \int_0^\infty d\sigma \int_0^1 dx_1 dx_2 \frac{\sigma}{\alpha_2 + \sigma + 4\xi(0)} \exp\left[-E_0(s, x_1)\alpha_2 - Q^2(s, x_1, E_0) \xi(0)\right] \\ & \cdot \exp\left\{-\left[\frac{m^2}{2A(0)} \frac{1-x_1}{x_1} + \frac{A(0)x_1\lambda_2}{2} (\lambda x_2(s + M^2 - m^2) + (1-2x_2)\lambda_2 s)\right] \sigma\right\} \end{aligned} \quad (5.25)$$

Consequently the corresponding weight function for the *two* identical vertex contributions becomes

$$\begin{aligned} \tilde{\rho}_V(E, s) \simeq & -2 \frac{g^2}{8\pi^2} A(0) \int_0^1 dx_1 dx_2 \Theta(E - E_0(s, x_1)) \exp\left[-Q^2(s, x_1, E) \xi(0)\right] \\ & \cdot \left[\frac{m^2}{2A(0)} \frac{1-x_1}{x_1} + \frac{A(0)x_1\lambda_2}{2} (\lambda x_2(s + M^2 - m^2) + (1-2x_2)\lambda_2 s)\right]^{-1}. \end{aligned} \quad (5.26)$$

The  $x_2$ -integral is the same as the one for combining denominators by the Feynman parameterization

$$\int_0^1 dx_2 \frac{1}{[a + bx_2]^2} = \frac{1}{ab} \quad (5.27)$$

and thus we obtain

$$\tilde{\rho}_V(E, s) \simeq -2 \frac{g^2}{8\pi^2} A(0) \int_0^1 dx_1 \Theta(E - E_0(s, x_1)) \frac{1}{EE_1(s, x_1, E)} \exp[-Q^2(s, x_1, E)\xi(0)] . \quad (5.28)$$

Combining all terms gives the simple formula

$$\tilde{\rho}(E, s) \simeq \frac{g^2}{8\pi^2} A(0) \int_0^1 dx_1 \Theta(E - E_0(s, x_1)) \left( \frac{1}{E} - \frac{1}{E_1(s, x_1, E)} \right)^2 \exp[-Q^2(s, x_1, E)\xi(0)] \quad (5.29)$$

which is evidently positive. This equation, together with Eq. (5.15), directly determines the imaginary part of the forward scattering amplitude. Hence one obtains a positive total cross section, as required. In the following, we shall first examine for which  $s$  this imaginary part first appears and subsequently shall derive an *analytical* expression for the total cross section at threshold.

## 5.2 Threshold Position

Let us now determine the threshold position. Eq. (5.29) should hold in the vicinity of the elastic threshold. Approaching it, the range of the  $x_1$ -integration shrinks due to the step function and is restricted to the interval  $x_1^{(-)} < x_1 < x_1^{(+)}$  where

$$x_1^{(\pm)} = \frac{1}{A(0)\lambda_2^2 s} \left[ E + \frac{m^2}{2A(0)} \pm \sqrt{\left( E + \frac{m^2}{2A(0)} \right)^2 - m^2 \lambda_2^2 s} \right] . \quad (5.30)$$

Exactly at threshold  $x_1^{(+)}$  and  $x_1^{(-)}$  coincide and only the minimum point

$$\bar{x}_1 = \frac{m}{A(0)\lambda_2\sqrt{s}} \quad (5.31)$$

is left over. Eq. (5.31) determines the lowest threshold position to be

$$E_{\text{thr.}} = \mathcal{D}(s_{\text{thr.}}) = E_0(\bar{x}_1, s_{\text{thr.}}) \quad (5.32)$$

or

$$E_0 = \lambda m \sqrt{s} - \frac{m^2}{2A(0)} . \quad (5.33)$$

which is the statement that that  $\tilde{\rho}(E, s)$  is only non-zero for  $E$  larger than  $E_0$ . Inserting Eq. (5.33) into Eq. (5.13), one finds the  $n^{\text{th}}$  threshold condition

$$n \left( 2 \lambda_2 m \sqrt{s_{\text{thr.}}} - \frac{m^2}{A(0)} \right) = \left[ 1 - (1 - \lambda_2)^2 \right] [s_{\text{thr.}} - \tilde{s}(s_{\text{thr.}})] . \quad (5.34)$$

The parameter  $\lambda_2$  is undetermined up to now. Certainly, one might try to fix it via the variational principle, which, however, in practice would seem to be rather difficult. An alternative, which is what

we shall do here, is to fix it by *demanding* that the lowest threshold (i.e.  $n = 1$ ) coincides exactly with  $\sqrt{s}_{\text{thr.}} = M + m$ .<sup>6</sup>

In order to solve for  $\lambda_2$ , we rewrite Eq. (5.34) as

$$\lambda_2^{(\pm)} = \frac{1}{M+m} \left[ M \pm \sqrt{M^2(1-\lambda)^2 + \frac{m^2}{A(0)} - \frac{\alpha M^2}{\pi} \Xi_p^1(s=(M+m)^2)} \right]. \quad (5.35)$$

As indicated, in general there are at least two solutions for  $\lambda_2$ . In fact, because  $\Xi_p^1$  also depends on  $\lambda_2$ , this equation is only implicit and actually may result in more than two solutions which have to be determined numerically. We have solved the implicit equation by iteration and found that below a critical coupling of about  $\alpha = 0.4$  each branch  $\lambda_2^{(+)}$  and  $\lambda_2^{(-)}$  yields exactly one solution. Above this coupling the solution for  $\lambda_2^{(+)}$  ceases to exist while at the same time the branch  $\lambda_2^{(-)}$  develops another solution. As the coupling is increased further, more solutions for  $\lambda_2^{(-)}$  come into existence.

Clearly, one needs to decide which one of these solutions corresponds to reality. For small couplings the decision seems relatively easy – the perturbative limit (in which  $\lambda = A(0) = 1$  and  $\tilde{s} = M^2$ ) of Eq. (5.35) is

$$\lambda_2^{(\pm)} = \frac{M \pm m}{M+m} + \mathcal{O}(\alpha) \quad . \quad (5.36)$$

As mentioned before, we require that in the limit of zero coupling the trial action becomes equal to the true action. Clearly only  $\lambda_2^{(+)}$  in the above equation satisfies this requirement, so we shall use this solution up to the critical coupling of  $\approx 0.4$ . Beyond this coupling we shall contend ourselves with using that value of  $\lambda_2^{(-)}$  which matches smoothly onto  $\lambda_2^{(+)}$  (only one of the solutions for  $\lambda_2^{(-)}$  has this property).

It is not entirely clear whether this is a satisfactory choice. In particular, one is naturally led to speculate whether this critical coupling actually has a physical meaning – perhaps the intermediate off-shell propagator feels the instability of the Wick-Cutkosky model already at smaller coupling constant than the on-shell propagator.<sup>7</sup> On the other hand, the division of solutions into  $\lambda_2^{(+)}$  and  $\lambda_2^{(-)}$  in Eq. (5.35) is somewhat artificial as, after all, this equation is only an implicit one for  $\lambda_2$ . Hence it is also possible that the critical coupling is just a mathematical artifact.

### 5.3 Total cross section

We now turn to the total cross section. Very close to threshold we can write

$$\begin{aligned} \tilde{\rho}(E, s) &\simeq \frac{g^2}{8\pi^2} A(0) \left( x_1^{(+)} - x_1^{(-)} \right) \left( \frac{1}{E} - \frac{1}{E_1(s_{\text{thr.}}, \bar{x}_1, E_0)} \right)^2 \exp \left[ -Q^2(s_{\text{thr.}}, \bar{x}_1, E_0) \xi(0) \right] \\ &\simeq \frac{g^2}{8\pi^2} \frac{2}{\lambda_2^2 (M+m)^2} \sqrt{[E - E_0(s_{\text{thr.}}, \bar{x}_1)] 2m\lambda_2(M+m)} e^{2m^2\xi(0)} \\ &\quad \cdot \left( \frac{1}{E_0(s_{\text{thr.}}, \bar{x}_1)} - \frac{1}{E_1(s_{\text{thr.}}, \bar{x}_1, E_0)} \right)^2 \end{aligned} \quad (5.37)$$

<sup>6</sup>Another alternative, again something which we do not pursue here, is to allow  $\lambda_2$  to become a function of  $s$  and hereby enforce all threshold positions to be precisely where they should be.

<sup>7</sup>We remind the reader that the variational equations for the on-shell propagator cease to have real solutions for couplings greater than about  $\alpha = 0.8$ , signaling the instability associated with this model.

where

$$E_0(s_{\text{thr.}}, \bar{x}_1) = m\lambda_2(M + m) - \frac{m^2}{2A_0} \equiv E_0 \quad (5.38)$$

$$E_1(s_{\text{thr.}}, \bar{x}_1, E_0) = m\lambda M - \frac{m^2}{2A_0} \equiv E_1. \quad (5.39)$$

The square root  $\sqrt{E - E_0}$  gives rise to a *linear* behaviour of the imaginary part of the amplitude with the three-momentum  $\mathbf{p}$  in the center-of-mass system as can be seen by expanding

$$s = \left( \sqrt{M^2 + \mathbf{p}^2} + \sqrt{m^2 + \mathbf{p}^2} \right)^2. \quad (5.40)$$

In contrast to the zeroth order variational approximation (III) where this behaviour was crucially dependent on the specific form of the retardation function at large values of  $\sigma$ , in first order this now holds for *all* parameterizations. This demonstrates the increased insensitivity of the first-order result to the variational *ansatz*. At threshold one obtains

$$\mathcal{I}m A(s_{\text{thr.}}, 0) = \frac{\alpha \mathcal{F}(s_{\text{thr.}}) M^2 e^{2m^2\xi(0)}}{\sqrt{(M+m)M} \lambda_2 m^2} \mathcal{Z} \frac{[\lambda_2 m + (\lambda_2 - \lambda)M]^2}{\left[ \lambda_2(M+m) - \frac{m}{2A(0)} \right]^2 \left( \lambda M - \frac{m}{2A(0)} \right)^2} p, \quad (5.41)$$

where the derivative in

$$\mathcal{Z} = \sqrt{2 - \lambda_2 - \frac{m}{m+M} - \frac{\alpha M^2}{\pi \lambda_2} \frac{d}{ds} \Xi_P^1(s)} \quad (5.42)$$

is to be evaluated at threshold. By the optical theorem the total cross section at threshold is obtained from  $\mathcal{I}m A(s, 0)$  using Eq. (5.2). It may readily be verified that this expression reduces to Eq. (5.7) in the perturbative limit.

## 6. Numerical Results

In Table 1 we collect the variational parameters determined from the variational equations at the pole of the propagator as well as the values for  $\lambda_2$  fixed at the lowest threshold. As usual we have taken  $M = 939$  MeV and  $m = 140$  MeV for the mass of the nucleon and meson, respectively. It should be noted that the parameters of the present ‘extended’ parameterizations are slightly different from those given in Ref. (III) because the variation now is not constrained to give the correct (zeroth order) thresholds. Consequently the minimum values of the variational functional are always lower than previously and are nearly identical with the full variational calculation (assuming no specific functional form for the retardation function), except at the largest coupling constant.

The total cross section at threshold is evaluated using the optical theorem and the analytic result of Eq. (5.41). The elastic cross section at threshold is determined by the real part of the scattering amplitude which is evaluated numerically. The ‘unitarity ratio’  $\sigma_{\text{el}}/\sigma_{\text{tot}}$  is shown in Fig. 4 for the allowed range of couplings. For comparison we include the results obtained in first order perturbation theory. As can be seen the variational result remains close to the unity whereas, as is well known, perturbation theory strongly violates it for large couplings.

	$\alpha = 0.1$	$\alpha = 0.2$	$\alpha = 0.3$	$\alpha = 0.4$	$\alpha = 0.5$	$\alpha = 0.6$	$\alpha = 0.7$	$\alpha = 0.8$
$y_1$	1.01142	1.01950	1.02899	1.04023	1.05405	1.07171	1.09755	1.15359
$y_2$	2.0702	2.3960	2.6302	2.8824	3.0850	3.1742	3.2194	3.1266
$\sqrt{w_1}$ [MeV]	636.09	612.10	587.31	560.04	530.05	496.02	453.33	381.08
$\sqrt{w_2}$ [MeV]	376.68	370.04	358.92	345.96	329.66	308.04	280.66	233.72
$\lambda$	0.97297	0.94390	0.91223	0.87718	0.83739	0.79032	0.72977	0.62361
$\lambda_2$	0.97690	0.95215	0.92534	0.89586	0.86273	0.82414	0.77587	0.69838
$A(0)$	1.01508	1.03213	1.05177	1.07489	1.10312	1.13951	1.19203	1.30393
$Z$	0.96087	0.91918	0.87429	0.82524	0.77045	0.70693	0.62748	0.49509
$\langle r^2 \rangle_0^{1/2}$ [fm]	0.0182	0.0258	0.0313	0.0352	0.0368	0.0327	-0.0164	-0.0886
$\langle r^2 \rangle_1^{1/2}$ [fm]	0.0481	0.0697	0.0879	0.1049	0.1220	0.1404	0.1623	0.1983

Table 1 : The variational parameters for the ‘ extended ’ retardation function writing  $C_1 = g^2 y_1 / (32\pi^2)$  and  $C_2 = y_2 m(m/M)^{3/2} \sqrt{\pi/2}$  and some derived quantities. A negative zeroth order rms-radius indicates that  $\langle r^2 \rangle_0 < 0$ .

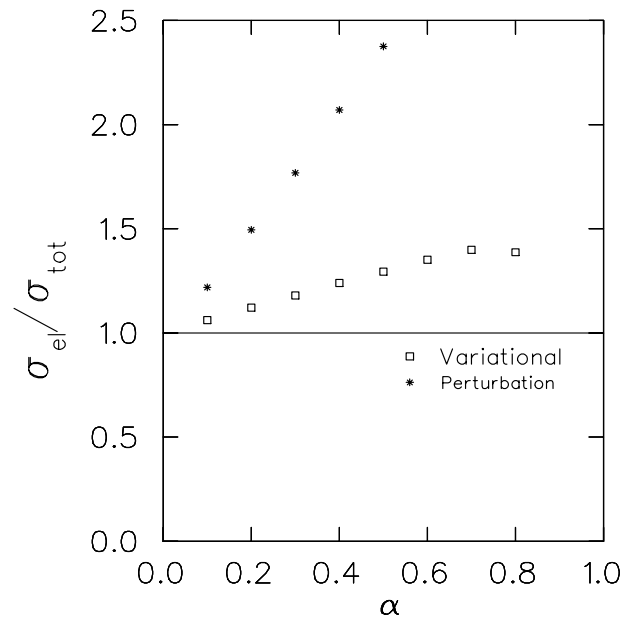


Figure 4: The unitarity ratio  $\sigma_{el}/\sigma_{tot}$  at threshold as a function of the coupling  $\alpha = g^2/(4\pi M^2)$ .

We also investigated the momentum dependence of the total cross section above the elastic, but below the first inelastic, threshold. For very small momenta one can apply Eq. (5.29) to obtain an analytic expression for the imaginary part of the forward scattering amplitude as a function of momentum as was done at threshold. In Fig. 5 we show the results for  $\alpha = 0.8$ . The results for the three lowest momenta are calculated analytically and they join nicely to the results obtained numerically at larger momenta. In contrast to what was observed for the vertex function in Ref. (IV), here one finds a smooth behaviour of the total cross section above threshold as a function of the momentum.

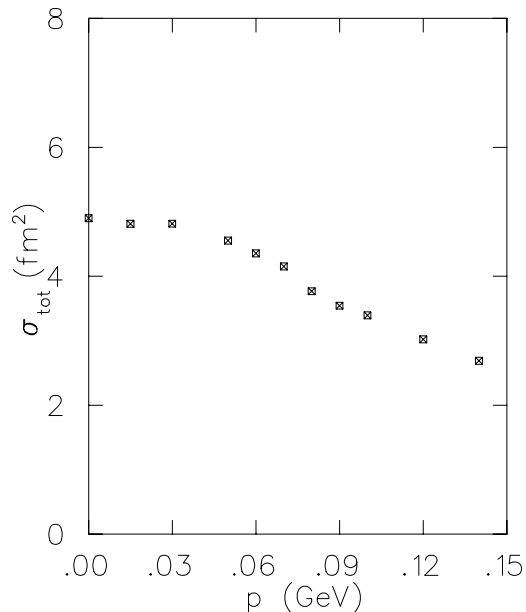


Figure 5: The total cross section as a function of the center-of-mass momentum  $|\mathbf{p}|$  at  $\alpha = 0.8$  .

## 7. Conclusions and Outlook

In this work Feynman’s variational method originally applied to the polaron problem, a non-relativistic field theory, was successfully generalized to study particle scattering in a relativistic setting. A central feature of the approach is that the variational principle is applied in the particle (or worldline) representation of field theory, making it rather similar to the non-relativistic theory. This is particularly so for the scalar theory under discussion in this paper – it is fair to characterise it as essentially Feynman’s polaron in  $4 + 1$  rather than  $3 + 1$  dimensions (with, in this case, phonons of non-zero mass).

The method amounts to a well-defined non-perturbative expansion of the Green functions of the theory. The leading term, which is the one calculated in this paper, obeys a *variational principle*. Higher order terms could be calculated as they have been for the polaron [29], if the need arose. Hence, roughly speaking, the “expansion parameter” is a dynamically determined quantity which adjusts itself in order to minimize the corrections due to these higher order terms. It is, of course,

crucial, that the starting point - the trial action - contains as much of the physics of the problem as possible. Although practically we are limited to quadratic (but *nonlocal*) trial actions there seems to be sufficient flexibility in the *ansatz* to achieve this goal. In the present work we even have generalized the previous trial action for better off-shell propagation without destroying the advantageous features of our method: the variational equations remain the same as previously, are independent of the number of external mesons and can be easily solved in Euclidean space.

In any expansion scheme such as this it is desirable that the lowest order term(s) are not only numerically reliable, but that the expansion also exhibits some of the analytic features of the full theory. A trivial illustration of this statement is relativistic invariance: both perturbation theory, for example, as well as the method outlined here are written in a manifestly invariant form. Also, crossing symmetry is maintained in both approaches. Another example, one that perturbation theory does not share with the present approach, is that the lowest order term already exhibits all the cuts and poles of the exact Green function.

A property of the theory which is connected with this, and which is maintained (at finite order) neither in the variational calculation nor in perturbation theory is the unitarity of the theory. In particular, the imaginary part of the forward scattering amplitude is connected to the total cross section via the optical theorem. Perturbation theory violates this very badly, something which is of course most obvious at tree level – here the imaginary part of the forward scattering cross section is identically zero because of the lack of analytic structure mentioned above. Because the variational calculation does not suffer from this deficiency one might suspect that unitarity is partially restored. The numerical results presented in this paper confirm this.

Although this is an important result in itself, restoration of unitarity was of course not the prime motivation for the work presented here. Rather, we were interested in the intrinsically non-perturbative nature of the variational method. For this reason we concentrated our attention on a kinematic region where non-perturbative effects are usually most important, namely near a threshold. We chose the lowest threshold because this did not require a calculation of higher-point Green functions.

The threshold region is important from another perspective as well. This region is sensitive to the infrared behaviour of the theory, while the fact that the theory is a divergent field theory means that ultraviolet physics plays a dominant role as well. The variational method is able to deal sensibly with both these regions simultaneously through the use of the profile function  $A(E)$  in the trial action, which is complementary to the retardation function  $f(\sigma)$ . Specifically, the ultraviolet (infrared) behaviour is simulated by the small- (large-)  $\sigma$  behaviour of this function which corresponds to the large- (small-)  $E$  behaviour of  $A(E)$ .

A difficulty with investigating the behaviour of the Green function near threshold is that although the variational approximation to the forward scattering amplitude does indeed contain cuts which one can identify with one, two etc. meson production in the intermediate state, the thresholds for these cuts are in general only approximately equal to their physical values. The solution of this problem which we chose illustrates another important feature of the variational method: although some properties of the exact Green function are reproduced for arbitrary trial actions, others may be enforced by restricting the form of the trial action. In particular, in the present work the new parameter  $\lambda_2$ , associated with the internal nucleon line, was fixed so that the lowest threshold was identical to the physical one.

This is certainly a legitimate procedure, although it would be more satisfying (and one would expect the numerical results to improve) if the variational principle itself would provide the correct thresholds. This would mean, in the context of our trial action, treating  $\lambda_2$  as a variational parameter with the daunting task of solving the variational equations for this parameter. We have chosen not to go into this direction but rather concentrate our efforts on a generalization of the present approach to a more realistic field theory, namely Quantum Electrodynamics.

**Acknowledgement:** We thank Nadia Fettes for a careful reading of the manuscript.

## References

- [1] R. P. Feynman, Phys. Rev. **97** (1955), 660.
- [2] R. P. Feynman and A. R. Hibbs: *Quantum Mechanics and Path Integrals*, McGraw-Hill (1965).
- [3] C. Alexandrou and R. Rosenfelder, Phys. Rep. **215** (1992) 1.
- [4] R. Rosenfelder, J. Phys. **A 27** (1994) 3523; C. Alexandrou, in: *Polarons and Applications*, ed. V. D. Lakhno, John Wiley and Sons (1994) 327; C. Alexandrou, Y. Lu and R. Rosenfelder, Z. Phys. **A 350** (1994) 131
- [5] C. Alexandrou and F. K. Diakonov, Z. Phys. **A 353** (1995) 149.
- [6] T. Barnes and G. I. Ghandour, Phys. Rev. **D 22** (1980) 924; P. M. Stevenson, Phys. Rev. **D 30** (1984) 1712, **D 32** (1985) 1389.
- [7] V. Fock, Phys. Zeit. Sow. **12** (1937) 404.
- [8] Y. Nambu, Prog. Theor. Phys. **5** (1950) 82.
- [9] R. P. Feynman, Phys. Rev. **80** (1950) 440.
- [10] J. Schwinger, Phys. Rev. **82** (1951) 664.
- [11] R. Rosenfelder and A. W. Schreiber, Phys. Rev. **D 53** (1996) 3337.
- [12] R. Rosenfelder and A. W. Schreiber, Phys. Rev. **D 53** (1996) 3354.
- [13] A. W. Schreiber, R. Rosenfelder and C. Alexandrou, to appear in Int. J. Mod. Phys. **E**, nucl-th/9504053.
- [14] A. W. Schreiber and R. Rosenfelder, Nucl. Phys. **A 601** (1996) 397.

- [15] G. C. Wick, Phys. Rev. **96** (1954) 1124.
- [16] R. E. Cutkosky, Phys. Rev. **96** (1954) 1135.
- [17] Yu. A. Simonov and J. A. Tjon, Ann. Phys. **228** (1993) 1.
- [18] T. Nieuwenhuis, J. A. Tjon and Yu. A. Simonov, contribution to the Few-Body Conference XIV, Amsterdam, 23 – 27 August 1993, p. 158; T. Nieuwenhuis and J. A. Tjon, Phys. Rev. Lett. **77** (1996) 814.
- [19] L. Di Leo and J. W. Darewych, Can. J. Phys. **70** (1992) 412; **71** (1993) 365.
- [20] M. Sawicki, Phys. Rev. **D 32** (1985) 2666.
- [21] J. R. Hiller, Phys. Rev. **D 44** (1991) 2504.
- [22] J. J. Wivoda and J. R. Hiller, Phys. Rev. **D 47** (1993) 4647.
- [23] C.-R. Ji, Phys. Lett. **B 322** (1994) 389.
- [24] C. Alexandrou, R. Rosenfelder and A. W. Schreiber, in preparation.
- [25] R. Rosenfelder, contribution to the 5<sup>th</sup> International Conference on Path Integrals from meV to MeV, Dubna, 27 – 31 May 1996, preprint PSI-PR-96-17.
- [26] R. P. Feynman, in: *Proc. of the Intern. Workshop on Variational Calculations in Quantum Field Theory*, L. Polley and D. E. L. Pottinger, eds., World Scientific (1988).
- [27] G. Baym, Phys. Rev. **117**, 886 (1960).
- [28] A. Erdélyi *et al.*: *Tables of Integral Transforms*, vol. 1, McGraw-Hill, New York (1954).
- [29] J. T. Marshall and L. R. Mills, Phys. Rev. **B 2** (1970) 3143; Y. Lu and R. Rosenfelder, Phys. Rev. **B 46** (1992) 5211.